

COUPLING IMPEDANCE BETWEEN PLANAR COILS INSIDE A LAYERED MEDIA

C. Carretero

Dep. Ing. Electrónica y Comunicaciones
Universidad de Zaragoza, María de Luna 1, Zaragoza 50018, Spain

R. Alonso

Dep. Física Aplicada
Universidad de Zaragoza, Pedro Cerbuna 12, Zaragoza 50009, Spain

J. Acero and J. M. Burdío

Dep. Ing. Electrónica y Comunicaciones
Universidad de Zaragoza, María de Luna 1, Zaragoza 50018, Spain

Abstract—In this paper a semi-analytical representation of the coupling impedance between coils composed of filamentary turns located between two layered media is provided on the basis of the spectral expansion of the fields involved in the system. Both media are composed of several layers of homogeneous materials characterized by their physical properties occupying, respectively, a half-space bounded by a plane. The domain in the middle, where the coils are placed, has vacuum properties. The development is focused on misaligned circular coils placed in parallel planes with respect to the media boundaries. Two different behavioral descriptions have been considered: first, the system is made up entirely of magnetic insulators and the coupling impedance is therefore purely inductive; second, at least one medium is an electrical conductor and, as a consequence, an additional resistive component emerges when the coupling impedance is evaluated. In the latter case, the coupling impedance exhibits a frequency dependence due to the dispersive effects associated with the induced currents generated in the conductive media. The model developed is verified by means of a comparison between numerical and experimental results.

Received 29 November 2010, Accepted 12 January 2011, Scheduled 25 January 2011
Corresponding author: Claudio Carretero (ccar@unizar.es).

1. INTRODUCTION

The model of a system composed of several planar coils inside a layered media is of interest for several applications, such as induction heating systems or contactless energy transfer systems. A closed form expression of the mutual impedance between two common axis circular turns immersed in air based on elliptic functions was firstly provided by Maxwell [1]. Several studies on two planar coils with parallel axes have been carried out by various authors [2–7]. These are particularly useful in applications concerning contactless energy transfer [8–13].

The equivalent impedance of planar coils can be modified by the presence of additional media, for instance, self-inductance of a single coil increases when a magnetic non-conductive layer is added [14]. Besides, where induced currents are driven in conductive media, the equivalent coil impedance is modified by an additional resistive contribution [15] due to power losses originated by this type of current. This is the basis of inductive heating system [16–18]. Mutual impedance between coils is also modified by the layered media. It should also be noted that resistive coupling occurs in the presence of at least one conductive layer, as is shown in studies concerning the coupling of two circular turns located between two half-space media [19] or the coupling between two ring-type coils above a half-space conductive medium [20].

The basic structure modeling the system considered in the analysis is depicted in Fig. 1. The j th coil represents the field source and the i th coil is the coupled coil. The layered media consist of N layers. Each k th layer is characterized by its electrical conductivity σ_k , magnetic permeability μ_k , and thickness d_k .

2. COUPLING IMPEDANCE BETWEEN COILS

In this problem, the j th coil generates a variable electromagnetic field. Thus, an electromotive force (*emf*) V_{ij} is induced on each i th coil whose origin is the current I_j driven by the j th coil. The coupling impedance Z_{ij} is defined as the ratio between *emf* and the current which is the source of the field, as is expressed as follows

$$Z_{ij} = \frac{V_{ij}}{I_j} \Big|_{I_{k \neq j} = 0}. \quad (1)$$

In order to calculate the *emf* V_{ij} , it is useful to find the electromagnetic field for a coil placed inside a layered media characterized by their magnetic permeabilities μ_k and electric conductivities σ_k . The j th coil consists of several circular elementary

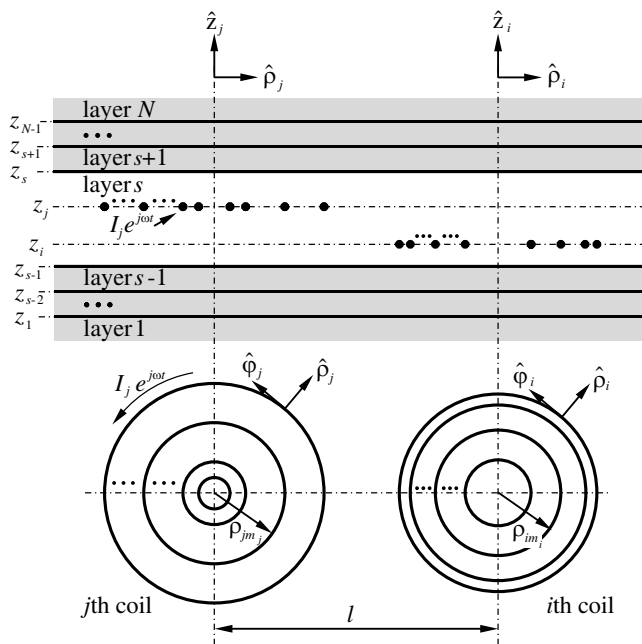


Figure 1. Two circular coils placed inside a layered media.

turns which possess a common axis directed to the normal direction of the boundaries. As a result, the equivalent impressed current density \mathbf{J}_j modeling the j th coil can be expressed in its coordinate system, as can be seen as follows

$$\mathbf{J}_j = I_j \cdot \sum_{m_j=1}^{n_j} \delta(z - z_{jm_j}) \delta(\rho - \rho_{jm_j}) \hat{\varphi}_j, \tag{2}$$

where ρ_{jm_j} is the radii and z_{jm_j} is the axial position of each turn, and I_j is the current driven by the j th coil.

In order to solve the system, a mixed potential point of view is adopted. Consider an impressed current density \mathbf{J}_e and a charge density ρ_e . Applying the Coulomb condition [21], the vector and scalar potentials in the harmonic formulation, where the exponential expression $e^{j\omega t}$ is disregarded for the sake of simplicity, satisfy the following equations

$$\nabla^2 \mathbf{A} - j\omega\sigma \mathbf{A} + \omega^2 \mu \epsilon \mathbf{A} = -\mu \mathbf{J}_e, \tag{3}$$

$$\nabla^2 \Phi = \frac{-j\omega}{\sigma + j\omega \epsilon} \rho_e. \tag{4}$$

In the case considered in this paper, the field sources are closed current loops without free charge densities. Therefore, the scalar potential Φ vanishes, and the fields can be represented by means of the magnetic vector potential \mathbf{A} . From [3] it is inferred that the fields arising from \mathbf{A} depends on the impressed current density \mathbf{J}_e , the divergenceless induced current density contribution $-j\omega\mu\sigma\mathbf{A}$ and the radiation term $\omega^2\mu\epsilon\mathbf{A}$.

In order to obtain the electric and magnetic field for a coil placed in a layered media some simplifications have been assumed. The effects of radiation have been neglected due to the fact that the wavelengths of the fields are much larger than the characteristic size of the system at the working frequencies considered. Thus, the quasistatic approach has been taken. To sum up, the following diffusion equation determines the fields

$$\nabla^2\mathbf{A} - j\omega\mu\sigma\mathbf{A} = -\mu\mathbf{J}_e. \quad (5)$$

2.1. Green's Function Solution

The solution of (5) can be worked out by means of the magnetic vector potential dyadic Green's function $\overline{\overline{\mathbf{G}}}(\mathbf{r}|\mathbf{r}')$ [22]

$$\mathbf{A}(\mathbf{r}) = \iiint \overline{\overline{\mathbf{G}}}(\mathbf{r}|\mathbf{r}')\mu\mathbf{J}(\mathbf{r}')dx'dy'dz'. \quad (6)$$

where the dyadic function $\overline{\overline{\mathbf{G}}}(\mathbf{r}|\mathbf{r}')$ satisfies the following expression [21]

$$\nabla^2\overline{\overline{\mathbf{G}}}(\mathbf{r}|\mathbf{r}') - j\omega\mu\sigma\overline{\overline{\mathbf{G}}}(\mathbf{r}|\mathbf{r}') = -\overline{\overline{\delta}}(\mathbf{r} - \mathbf{r}'). \quad (7)$$

The translational symmetry of the media with respect to the two transversal coordinates implies that $\overline{\overline{\mathbf{G}}}(\mathbf{r}|\mathbf{r}') = \overline{\overline{\mathbf{G}}}(\rho - \rho'; z, z')$. Applying the spectral decomposition to the transversal coordinates [23, 24], we have the equivalence

$$\overline{\overline{\mathbf{G}}}(\rho - \rho'; z, z') = \mathcal{F}^{-1}\overline{\overline{\mathbf{G}}}(\mathbf{k}_\rho; z, z'). \quad (8)$$

where \mathcal{F}^{-1} is the inverse spectral transform and \mathbf{k}_ρ is the bidimensional transformed variable of the spatial polar coordinate ρ .

Moreover, due to the multilayered geometry with parallel planar boundaries, the dyadic Green's function possesses a diagonal structure

$$\overline{\overline{\mathbf{G}}}(\mathbf{k}_\rho; z, z') = \begin{vmatrix} \tilde{G}_{xx} & 0 & 0 \\ 0 & \tilde{G}_{yy} & 0 \\ 0 & 0 & \tilde{G}_{zz} \end{vmatrix}. \quad (9)$$

Considering the axial symmetry, \tilde{G}_{xx} and \tilde{G}_{yy} have identical expressions named $G(\mathbf{k}_\rho; z, z')$. The third component \tilde{G}_{zz} is not

needed in our treatment because no field sources are directed in the axial direction. As a result, only the transformed Green's function $G(\mathbf{k}_\rho; z, z')$ is of interest for solving the system fields.

Performing the spectral decomposition in (7) for a linear, isotropic and homogeneous medium, the transformed Green's function $G(\mathbf{k}_\rho; z, z')$ obeys the following equation

$$\partial_z^2 G(\mathbf{k}_\rho; z, z') - (k_\rho^2 + j\omega\mu\sigma)G(\mathbf{k}_\rho; z, z') = -\delta(z - z'). \quad (10)$$

The general solution of the homogenous equation, can be expressed as

$$G(\mathbf{k}_\rho; z, z') = Ae^{\eta(z-z')} + Be^{-\eta(z-z')}. \quad (11)$$

where it is defined that $\eta = \sqrt{k_\rho^2 + j\omega\mu\sigma}$.

Introducing the solution provided in (11) into (10), and considering a medium with air properties, the spectral representation of the Green's function $G(\mathbf{k}_\rho; z, z')$ is equal to

$$G(\mathbf{k}_\rho; z, z') = \frac{1}{2k_\rho} e^{-k_\rho|z-z'|}. \quad (12)$$

The purpose of this work is to calculate the coupling between the coils placed in the layer s , which has the physical properties of vacuum. Therefore, we need to extract the fields in this layer originated by the j th coil including the multilayered structure effects. It should be noted that many authors give expressions for the Green's functions of a layered media [25–27], but these works use the complete electromagnetic description based on the solution of wave equations which describe systems dominated by propagation behavior. The combination of the wave solution and the phenomena associated with the interface between layers leads to the definition of the transmission and reflection coefficients. However, assuming the quasistatic approach, the electromagnetic field obeys the parabolic diffusion equation provided in (5) with spectral eigenfunctions simultaneously fixed in the overall space [28] which differ considerably from the wave solution.

Assuming that in each k th layer a solution of the type expressed in (11) is valid, the Green's function solution is obtained by applying the boundary conditions at the limits between contiguous layers. Moreover, the Green's function must be bounded, which implies the constraints $B_1 = 0$ and $A_N = 0$. The continuity in the transversal electric and magnetic field component can be expressed as

$$G_k(\mathbf{k}_\rho; z_k, z') = G_{k+1}(\mathbf{k}_\rho; z_k, z'), \quad (13)$$

$$\frac{\partial_z G_k(\mathbf{k}_\rho; z_k, z')}{\mu_k} = \frac{\partial_z G_{k+1}(\mathbf{k}_\rho; z_k, z')}{\mu_{k+1}}. \quad (14)$$

Or, equivalently, by introducing (11) into the two previous expressions and rearranging the results in a matrix notation, the following is obtained

$$\mathbf{M}_k(\mathbf{k}_\rho, d_k) \cdot \begin{vmatrix} A_k(\mathbf{k}_\rho) \\ B_k(\mathbf{k}_\rho) \end{vmatrix} = \mathbf{M}_{k+1}(\mathbf{k}_\rho, 0) \cdot \begin{vmatrix} A_{k+1}(\mathbf{k}_\rho) \\ B_{k+1}(\mathbf{k}_\rho) \end{vmatrix}, \quad (15)$$

where d_k is the thickness of the k th layer which is equal to $z_k - z_{k-1}$, and the matrix \mathbf{M}_k is defined as follows

$$\mathbf{M}_k(\mathbf{k}_\rho, d_k) = \begin{vmatrix} e^{\eta_k d_k} & e^{-\eta_k d_k} \\ \frac{\eta_k}{\mu_k} e^{\eta_k d_k} & -\frac{\eta_k}{\mu_k} e^{-\eta_k d_k} \end{vmatrix}. \quad (16)$$

Rearranging (15), the relationship between the coefficients of two contiguous layers can be expressed as follows

$$\begin{vmatrix} A_k(\mathbf{k}_\rho) \\ B_k(\mathbf{k}_\rho) \end{vmatrix} = \mathbf{R}_{k,k+1}(\mathbf{k}_\rho, d_k) \cdot \begin{vmatrix} A_{k+1}(\mathbf{k}_\rho) \\ B_{k+1}(\mathbf{k}_\rho) \end{vmatrix}, \quad (17)$$

where $\mathbf{R}_{k,k+1}(\mathbf{k}_\rho, d_k)$ is equal to $(\mathbf{M}_k(\mathbf{k}_\rho, d_k))^{-1} \cdot \mathbf{M}_{k+1}(\mathbf{k}_\rho, 0)$ or

$$\mathbf{R}_{k,k+1}(\mathbf{k}_\rho, d_k) = \frac{1}{2} \begin{vmatrix} (1 + \frac{\mu_k}{\eta_k} \frac{\eta_{k+1}}{\mu_{k+1}}) e^{-\eta_k d_k} & (1 - \frac{\mu_k}{\eta_k} \frac{\eta_{k+1}}{\mu_{k+1}}) e^{-\eta_k d_k} \\ (1 - \frac{\mu_k}{\eta_k} \frac{\eta_{k+1}}{\mu_{k+1}}) e^{\eta_k d_k} & (1 + \frac{\mu_k}{\eta_k} \frac{\eta_{k+1}}{\mu_{k+1}}) e^{\eta_k d_k} \end{vmatrix}. \quad (18)$$

In order to simplify the treatment, we consider that the axial position z' , where the source field is located, divides the domain s into two subspaces s^+ and s^- for positions above and below the source, respectively. Applying (17) recursively and including the constraint expressed as $A_N = 0$, the coefficients in the subdomain s^+ can be written as

$$\begin{vmatrix} A_s^+(\mathbf{k}_\rho) \\ B_s^+(\mathbf{k}_\rho) \end{vmatrix} = \prod_{k=s}^{N-1} \mathbf{R}_{k,k+1}(\mathbf{k}_\rho, d_k) \cdot \begin{vmatrix} 0 \\ B_N(\mathbf{k}_\rho) \end{vmatrix}, \quad (19)$$

where d_s is equal to zero because the coefficients are evaluated in the upper boundary at the z_s position of the subdomain s^+ .

Note that the matrix product of $\mathbf{R}_{k,k+1}(\mathbf{k}_\rho, d_k)$ for k ranging from s to $N - 1$ is a 2×2 elements matrix because each $\mathbf{R}_{k,k+1}(\mathbf{k}_\rho, d_k)$ is a 2×2 square matrix, as it can be seen in (18). Therefore, the matrix $\mathbf{T}^+(\mathbf{k}_\rho)$ is defined for mathematical purposes as follows

$$\mathbf{T}^+(\mathbf{k}_\rho) = \begin{vmatrix} T_{11}^+(\mathbf{k}_\rho) & T_{12}^+(\mathbf{k}_\rho) \\ T_{21}^+(\mathbf{k}_\rho) & T_{22}^+(\mathbf{k}_\rho) \end{vmatrix} = \prod_{k=s}^{N-1} \mathbf{R}_{k,k+1}(\mathbf{k}_\rho, d_k). \quad (20)$$

Considering that A_N is zero, the product between the matrix $\mathbf{T}^+(\mathbf{k}_\rho)$ and the vector of coefficients when (20) is introduced into (19) leads to a the following expression

$$\begin{vmatrix} A_s^+(\mathbf{k}_\rho) \\ B_s^+(\mathbf{k}_\rho) \end{vmatrix} = \begin{vmatrix} T_{12}^+(\mathbf{k}_\rho) \\ T_{22}^+(\mathbf{k}_\rho) \end{vmatrix} \cdot B_N(\mathbf{k}_\rho). \quad (21)$$

The coefficients A_s^+ and B_s^+ are equal to the product between the coefficient B_N and a single matrix $\mathbf{T}^+(\mathbf{k}_\rho)$ element, T_{12}^+ and T_{22}^+ , respectively. Consequently, the latter expression can be rearranged to obtain the following relationship between the coefficients A_s^+ and B_s^+

$$A_s^+(\mathbf{k}_\rho) = \phi^+(\mathbf{k}_\rho) \cdot B_s^+(\mathbf{k}_\rho), \tag{22}$$

where $\phi^+(\mathbf{k}_\rho)$ can be written as

$$\phi^+(\mathbf{k}_\rho) = \frac{T_{12}^+(\mathbf{k}_\rho)}{T_{22}^+(\mathbf{k}_\rho)}. \tag{23}$$

In the same way as appear in (22) for the subdomain s^- , we can write

$$B_s^-(\mathbf{k}_\rho) = \phi^-(\mathbf{k}_\rho) \cdot A_s^-(\mathbf{k}_\rho), \tag{24}$$

where $\phi^-(\mathbf{k}_\rho)$ is given by

$$\phi^-(\mathbf{k}_\rho) = \frac{T_{21}^-(\mathbf{k}_\rho)}{T_{11}^-(\mathbf{k}_\rho)}, \tag{25}$$

and the matrix $\mathbf{T}^-(\mathbf{k}_\rho)$ is defined as

$$\mathbf{T}^-(\mathbf{k}_\rho) = \prod_{k=1}^{s-1} \mathbf{R}_{k+1,k}(\mathbf{k}_\rho, d_k), \tag{26}$$

where $\mathbf{R}_{k+1,k}(\mathbf{k}_\rho, d_k)$ is equal to $\mathbf{R}_{k,k+1}(\mathbf{k}_\rho, -d_k)$.

It is worth noting that, as can be seen in (22), the field contribution associated with the coefficient $A_s^+(\mathbf{k}_\rho)$, is due to the effects originated in the layered media as a response to the excitation of the field accounted for the coefficient $B_s^+(\mathbf{k}_\rho)$.

The field component associated to $B_s^+(\mathbf{k}_\rho)$ arises from the sources located below the subdomain s^+ due to the impressed current at the position z' and the effects of the lower layered media located under the subdomain s^- . Thus, considering (11), (12) and the field continuity condition, we have

$$B_s^+(\mathbf{k}_\rho)e^{-k_\rho(z-z_s)} = \frac{e^{-k_\rho(z-z')}}{2k_\rho} + B_s^-(\mathbf{k}_\rho)e^{-k_\rho(z-z_{s-1})} \quad \text{if } z \in s^+. \tag{27}$$

Similarly, the coefficient $A_s^-(\mathbf{k}_\rho)$ obeys

$$A_s^-(\mathbf{k}_\rho)e^{k_\rho(z-z_{s-1})} = \frac{e^{k_\rho(z-z')}}{2k_\rho} + A_s^+(\mathbf{k}_\rho, z_s)e^{k_\rho(z-z_s)} \quad \text{if } z \in s^-. \tag{28}$$

As a result, from the aforementioned results, applying (22) and (24), and performing the appropriate operations, we obtain

$$G(\mathbf{k}_\rho, z, z') = \frac{1}{2k_\rho} \left[e^{-k_\rho |\Delta z|} + \frac{e^{-k_\rho d'_u} + \phi^- e^{-k_\rho (d'_u + 2d'_l)}}{1 - \phi^- \phi^+ e^{-2k_\rho (d'_u + d'_l)}} \phi^+ e^{-k_\rho d_u} + \frac{e^{-k_\rho d'_l} + \phi^+ e^{-k_\rho (2d'_u + d'_l)}}{1 - \phi^- \phi^+ e^{-2k_\rho (d'_u + d'_l)}} \phi^- e^{-k_\rho d_l} \right] \text{ if } z \in s. \quad (29)$$

where Δz , d_u , d_l , d'_u and d'_l represent the distances $z - z'$, $z_s - z$, $z - z_{s-1}$, $z_s - z'$ and $z' - z_{s-1}$, respectively. The \mathbf{k}_ρ dependence of $\phi^-(\mathbf{k}_\rho)$ and $\phi^+(\mathbf{k}_\rho)$ is implicitly assumed.

2.2. Coupling Impedance between Coils

Introducing the previous results into (6), the spectral representation of the magnetic vector potential $\mathbf{A}(\mathbf{k}_\rho, z)$ can be written in the following form

$$\mathbf{A}(\mathbf{k}_\rho, z) = \int_{-\infty}^{\infty} G(\mathbf{k}_\rho, z, z') \mu_0 \mathbf{J}_e(\mathbf{k}_\rho, z') dz'. \quad (30)$$

The solution thereby depends on the physical multilayered structure through the Green's function $G(\mathbf{k}_\rho; z, z')$, and the spectral representation of the impressed current density distribution $\mathbf{J}_e(\mathbf{k}_\rho, z')$. In this case the latter one corresponds to the current \mathbf{J}_j driven by the j th coil. The correct framework to obtain the bidimensional Fourier Transform of the current distribution \mathbf{J}_j provided in (2) corresponds to the Vector Hankel Transform [29] which defines the Fourier Transform in polar coordinates, as can be seen as follows

$$\mathbf{J}_j(\mathbf{k}_\rho, z') = \sum_{n=-\infty}^{\infty} e^{-jnk_\varphi} \int_0^{\infty} \bar{\bar{\mathbf{J}}}_n(k_\rho \rho) \cdot \mathbf{J}_{j,n}(\rho, z') \rho d\rho, \quad (31)$$

where $\bar{\bar{\mathbf{J}}}_n(k_\rho \rho)$ is a Bessel function dependant 2×2 matrix

$$\bar{\bar{\mathbf{J}}}_n(k_\rho \rho) = \begin{vmatrix} J'_n(k_\rho \rho) & -\frac{in}{k_\rho \rho} J_n(k_\rho \rho) \\ \frac{in}{k_\rho \rho} J_n(k_\rho \rho) & J'_n(k_\rho \rho) \end{vmatrix}. \quad (32)$$

Owing to the axial symmetry, the series consists of a single transformed term $n = 0$ equal to the original expression. In this case, the expression (32) is a diagonal matrix whose non-null terms are equal to the first degree Bessel function $-J_1(k_{\rho_j} \rho_j)$. Moreover, since the non-null vectorial coefficient is directed along the azimuthal direction, the Vector Hankel Transform (31) can be expressed as

$$\mathbf{J}_j(\mathbf{k}_\rho, z') = - \int_0^{\infty} \rho J_1(k_\rho \rho) \mathbf{J}_j(\rho, z') d\rho \hat{\mathbf{k}}_\rho, \quad (33)$$

and introducing the spatial representation of the current distribution $\mathbf{J}_j(\mathbf{r})$ provided in (2), this leads to

$$\mathbf{J}_j(\mathbf{k}_\rho, z') = -I_j \delta(z' - z_j) \sum_{m_j=1}^{n_j} \rho_{jm_j} J_1(k_\rho \rho_{jm_j}) \hat{\mathbf{k}}_\varphi. \quad (34)$$

Considering the expression (30) for a coil with turns placed in the same plane at z_j , we have

$$\mathbf{A}_j(\mathbf{k}_\rho, z) = -\mu_0 I_j G(\mathbf{k}_\rho, z, z_j) \sum_{m_j=1}^{n_j} \rho_{jm_j} J_1(k_\rho \rho_{jm_j}) \hat{\mathbf{k}}_\varphi. \quad (35)$$

It should be noted that the Green's function spectral representation $G(\mathbf{k}_{\rho_j}; z, z')$ depends only on the amplitude of the transformed variable \mathbf{k}_{ρ_j} , and, it can therefore be rewritten as $G(k_{\rho_j}; z, z')$.

Applying the inverse Vector Hankel Transform, the spatial formulation of the magnetic vector potential $\mathbf{A}_j(\mathbf{r})$ is defined by

$$\mathbf{A}_j(\mathbf{r}) = \mu_0 I_j \int_0^\infty G(k_\rho, z, z_j) \cdot \sum_{m_j=1}^{n_j} \rho_{jm_j} J_1(k_\rho \rho_{jm_j}) J_1(k_\rho \rho) k_\rho dk_\rho \hat{\varphi}. \quad (36)$$

The *emf* V_{ij} induced in the i th coil can be calculated by integrating the electric field $\mathbf{E}_j(\mathbf{r}) = -j\omega \mathbf{A}_j(\mathbf{r})$ arising from the j th coil along its turn trajectories. Therefore, we have

$$\begin{aligned} V_{ij} = & j\omega \mu_0 I_j \sum_{m_i=1}^{n_i} \oint_{C_{turn\ i\ m_i}} \int_0^\infty G(k_\rho, z_i, z_j) \\ & \cdot \sum_{m_j=1}^{n_j} \rho_{jm_j} J_1(k_\rho \rho_{im_i}) J_1(k_\rho \rho_{jm_j}) k_\rho dk_\rho \hat{\varphi}_j \cdot d\mathbf{r}_{im_i}. \end{aligned} \quad (37)$$

Given that the turns of the i th coil consist of circular closed loops with a common axis, the differential trajectory element $d\mathbf{r}_{im_i}$ is equivalent to $\rho_{im_i} \hat{\varphi}_i d\varphi_i$ and the integral ranges from 0 to 2π . As a result, (37) can be expressed as follows

$$\begin{aligned} V_{ij} = & j\omega \mu_0 I_j \int_0^{2\pi} \int_0^\infty G(k_\rho, z_i, z_j) \\ & \cdot \sum_{m_i=1}^{n_i} \sum_{m_j=1}^{n_j} \rho_{im_i} \rho_{jm_j} J_1(k_\rho \rho_{im_i}) J_1(k_\rho \rho_{jm_j}) (\hat{\varphi}_i \cdot \hat{\varphi}_j) k_\rho dk_\rho d\varphi_i. \end{aligned} \quad (38)$$

From the geometrical relationship between both coordinate systems, it is possible to establish the following transformations

$$\rho_j = \sqrt{\rho_i^2 + 2l\rho_i \cos \varphi_i + l^2}, \tag{39}$$

$$\hat{\varphi}_i \cdot \hat{\varphi}_j = \frac{\rho_i + l \cos \varphi_i}{\sqrt{\rho_i^2 + 2l\rho_i \cos \varphi_i + l^2}}. \tag{40}$$

Thus, Equation (38) becomes

$$V_{ij} = j\omega\mu_0 I_j \int_0^\infty G(k_\rho, z_i, z_j) \sum_{m_i=1}^{n_i} \sum_{m_j=1}^{n_j} \rho_{im_i} J_1(k_\rho \rho_{im_i}) \cdot \int_0^{2\pi} \frac{J_1\left(k_\rho \sqrt{\rho_{im_i}^2 + 2l\rho_{im_i} \cos \varphi_i + l^2}\right)}{\sqrt{\rho_{im_i}^2 + 2l\rho_{im_i} \cos \varphi_i + l^2}} (\rho_{im_i} + l \cos \varphi_i) d\varphi_i k_\rho dk_\rho. \tag{41}$$

where the second integral term in (41) is equivalent to the following expression

$$-\frac{1}{k_\rho} \frac{\partial}{\partial \rho_{im_i}} \int_0^{2\pi} J_0(k_\rho \sqrt{\rho_{im_i}^2 + 2l\rho_{im_i} \cos \varphi_i + l^2}) d\varphi_i. \tag{42}$$

The integrand in (42) can be expanded by using Graf’s addition theorem

$$J_0(k_\rho \sqrt{\rho_{im_i}^2 + 2l\rho_{im_i} \cos \varphi_i + l^2}) = J_0(k_\rho \rho_{im_i}) J_0(k_\rho l) + \sum_{n=1}^\infty J_n(k_\rho \rho_{im_i}) J_n(k_\rho l) \cos(n\varphi_i). \tag{43}$$

Note that only the first term contributes to the integral because the cosine dependent terms vanish when integration is performed in the azimuthal variable φ_i . Consequently, (41) can be expressed as

$$V_{ij} = j\omega\mu_0 I_j \int_0^\infty G(k_\rho, z_i, z_j) \sum_{m_i=1}^{n_i} \sum_{m_j=1}^{n_j} 2\pi \rho_{im_i} \rho_{jm_j} \cdot J_1(k_\rho \rho_{im_i}) J_1(k_\rho \rho_{jm_j}) J_0(k_\rho l) k_\rho dk_\rho. \tag{44}$$

The coupling impedance Z_{ij} is defined as the ratio between the

induced *emf* V_{ij} and the current I_j . Consequently, from (29) we have

$$\begin{aligned}
 Z_{ij} = & j\omega\mu_0\pi \int_0^\infty \left[e^{-k_\rho|d_{ij}|} + \frac{e^{-2k_\rho d_{uj}} + \phi^- e^{-2k_\rho(d_{uj}+d_{lj})}}{1 - \phi^- \phi^+ e^{-2k_\rho(d_{uj}+d_{lj})}} \phi^+ e^{k_\rho d_{ij}} \right. \\
 & \left. + \frac{e^{-2k_\rho d_{lj}} + \phi^+ e^{-2k_\rho(d_{uj}+d_{lj})}}{1 - \phi^- \phi^+ e^{-2k_\rho(d_{uj}+d_{lj})}} \phi^- e^{-k_\rho d_{ij}} \right] \\
 & \cdot \sum_{m_i=1}^{n_i} \sum_{m_j=1}^{n_i} \rho_{im_i} \rho_{jm_j} J_1(k_\rho \rho_{im_i}) J_1(k_\rho \rho_{im_j}) J_0(k_\rho l) dk_\rho. \quad (45)
 \end{aligned}$$

where d_{ij} , d_{uj} and d_{lj} represent $z_i - z_j$, $z_s - z_j$ and $z_j - z_{s-1}$.

3. EXPERIMENTAL RESULTS

An experimental setup based on the structure depicted in Fig. 1 has been built to verify the models. The system impedances have been measured by means of a precision LCR meter (Agilent E4980A). The coils tested are two identical planar windings of 5 circular turns equally spaced with radii between 21 and 32 mm made in a printed circuit board (PCB). The coils can be modeled as filamentary currents because all the turns possess a small cross-section area.

Two different configurations have been tested in order to verify the developed coupling expressions between two coils. The first consists of two parallel coils placed between two magnetic media, which is the basic structure used for energy transfer purposes. Additionally, an arrangement suitable for induction heating purposes, where the upper media is an electric conductor material usually called the load, has been evaluated to validate the mutual coupling expressions.

The high-precision LCR-meter does not allow simultaneous measurements of current I_j in the j th coil and *emf* V_i in the i th coil. Therefore, the process to obtain each experimental value consists of two different measures. Moreover, the procedure to evaluate the coupling impedance exploits the reciprocity theorem [24, 30], whose main consequence is a symmetric impedance matrix or, equivalently, $Z_{ij} = Z_{ji}$. In the first measurement, the coils are connected in an in-phase series configuration in order to inject the same current into both coils. The impedance $Z_{in} = Z_{ii} + Z_{jj} + Z_{ij} + Z_{ji}$ was thus directly obtained. Next, an opposite-phase series configuration was measured, obtaining $Z_{opp} = Z_{ii} + Z_{jj} - Z_{ij} - Z_{ji}$. Finally, cross coefficients have been quantified because $Z_{ij} = \frac{Z_{in} - Z_{opp}}{4}$.

3.1. Parallel Coils between Two Magnetic Layered Insulators

In this configuration, the two media are made with an insulator material, such as ferrite, characterized by a magnetic permeability $\mu_r = 2000$. Both layered media are of identical thickness $t = 4.5$ mm. The distance between the two media is $d_{lu} = 8.25$ mm. The coils are supported in the internal sides of each ferrite layer at a distance equal to the PCB thickness. Thus, the distance between the lower media and the i th coil is $d_{li} = 1.75$ mm, the distance between the j th coil and the upper media is $d_{uj} = 1.75$ mm and the distance between the axial position of the coils is $d_{ij} = 5.75$ mm.

It should be noted that, in a contactless energy transfer system, the objective of the magnetic media is coupling enhancement between coils so as to improve the system performance.

The measurements have been carried out at different distances l between coil axes uniformly spaced from 0 to 60 mm, as shown in Fig. 2. The mutual inductance L_{ij} decreases when the coils are misaligned up to a distance l where L_{ij} becomes slightly negative, and vanishes for a larger distance, as shown in Fig. 2.

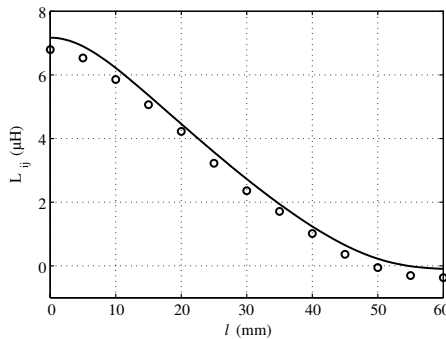


Figure 2. Coupling inductance for two coils located between two ferrite layers. Experimental data measurements (circular symbol) and analytical results (continuous line) are represented.

3.2. Coplanar Coils at a Distance between Axes $l = 70$ mm

The second configuration has been built by placing both coils over a ferrite layer at the same distances d_{li} and d_{lj} of 1.75 mm, the distance l between their axes being equal to 70 mm. The upper media, called the load, is a plate located above the lower media at a distance $d_{lu} = 8.25$ mm. Three different materials have been placed in the

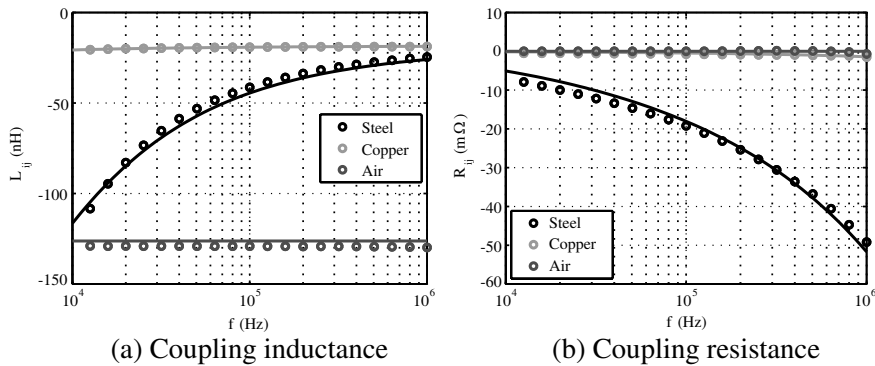


Figure 3. Frequency dependence of the coupling impedance for three different upper layers.

position of the upper media: ferromagnetic steel, copper and air. Ferromagnetic steel is characterized by a conductivity $\sigma = 8 \cdot 10^6$ S/m and a magnetic permeability $\mu_r = 150$, copper by a conductivity $\sigma = 5.8 \cdot 10^7$ S/m and a unitary relative permeability, and air by its non-magnetic insulator properties. The two first loads correspond to the typical composition of an induction heating load, and can therefore be considered as the induction reference load. The last is equivalent to a non-loaded system. The measurements have been performed for a frequency set ranging from 10 kHz to 1 MHz and the results obtained are shown in Fig. 3.

4. CONCLUSIONS

A semi-analytical solution for coupling impedances between non-coaxial rounded planar coils placed inside a multilayered media has been explained in this paper.

As a result, a full description of the electric behavior of a multi-coil system can be obtained from this solution. A simpler system consisting of a single coil has been extensively studied in previous works, but its electric equivalent impedance can be easily inferred from this model considering the self-impedance as a coupling impedance between two identical coils placed in the same position, partially proving its validity. For a multi-coil system the remaining additional terms can be calculated individually as single coupling terms. Therefore, it is possible to optimize systems using this structure on the basis of the study performed.

Finally, the analytical expressions obtained have been experimen-

tally validated for the two basic structures considered in order to verify the usefulness of the model in practical applications. The measurement results are in good agreement with the analytical results.

ACKNOWLEDGMENT

This work was partly supported by the Spanish MEC under Project CSD2009-00046 and Project TEC2010-19207, by the DGA under Project PI065/09, and by the Bosch and Siemens Home Appliances Group.

REFERENCES

1. Maxwell, J. C., *A Treatise on Electricity and Magnetism*, Dover, New York, 1954 (reprint from the original from 1891).
2. Babic, S. I., F. Sirois, and C. Akyel, "Validity check of mutual inductance formulas for circular filaments with lateral and angular misalignments," *Progress In Electromagnetics Research M*, Vol. 8, 15–26, 2009.
3. Akyel, C., S. I. Babic, and M.-M. Mahmoudi, "Mutual inductance calculation for non-coaxial circular air coils with parallel axes," *Progress In Electromagnetics Research*, Vol. 91, 287–301, 2009.
4. Conway, J. T., "Noncoaxial inductance calculations without the vector potential for axisymmetric coils and planar coils," *IEEE Trans. Magn.*, Vol. 44, No. 4, 453–462, 2008.
5. Conway, J. T., "Inductance calculations for circular coils of rectangular cross section and parallel axes using bessel and struve functions," *IEEE Trans. Magn.*, Vol. 46, No. 1, 75–81, 2010.
6. Ravaud, R., G. Lemarquand, V. Lemarquand, S. I. Babic, and C. Akyel, "Mutual inductance and force exerted between thick coils," *Progress In Electromagnetics Research*, Vol. 102, 367–380, 2010.
7. Ravaud, R., et al., "Cylindrical magnets and coils: Fields, forces and inductances," *IEEE Trans. Magn.*, Vol. 46, No. 9, 3585–3590, 2010.
8. Zierhofer, C. M. and E. S. Hochmair, "Geometric approach for coupling enhancement of magnetically coupled coils," *IEEE Trans. Biomed. Eng.*, Vol. 43, No. 7, 704–714, 1996.
9. Soma, M., D. C. Galbraith, and R. L. White, "Radio-frequency coils in implantable devices: misalignment analysis and design procedure," *IEEE Trans. Biomed. Eng.*, Vol. 34, No. 4, 276–282, 1987.

10. Costa, E. M. M., "Planar transformers excited by square waves," *Progress In Electromagnetics Research*, Vol. 100, 55–68, 2010.
11. Peng, L., O. Breinbjerg, and N. A. Mortensen, "Wireless energy transfer through non-resonant magnetic coupling," *Journal of Electromagnetic Waves and Applications*, Vol. 24, Nos. 11–12, 1587–1598, 2010.
12. Wei, X. C., E. P. Li, Y. L. Guan, and Y. H. Chong, "Simulation and experimental comparison of different coupling mechanism for the wireless electricity transfer," *Journal of Electromagnetic Waves and Applications*, Vol. 23, No. 7, 925–934, 2009.
13. Su, Y. P., L. Xun, and S. Y. R. Hui, "Mutual inductance calculation of movable planar coils on parallel surfaces," *IEEE Trans. Power Electron.*, Vol. 24, No. 4, 1115–1123, 2009.
14. Roshen, W. A., "Analysis of planar sandwich inductors by current images," *IEEE Trans. Magn.*, Vol. 26, No. 5, 2880–2887, 1990.
15. Luquire, J. W., W. E. Deeds, and C. V. Dodd, "Alternating current distribution between planar conductors," *J. Appl. Phys.*, Vol. 41, No. 10, 3983–3991, 1970.
16. Hurley, W. G. and M. C. Duffy, "Calculation of self- and mutual impedances in planar sandwich inductors," *IEEE Trans. Magn.*, Vol. 33, No. 3, 2282–2290, 1997.
17. Acero, J., et al., "Modeling of planar spiral inductors between two multilayer media for induction heating applications," *IEEE Trans. Magn.*, Vol. 42, No. 11, 3719–3729, 2006.
18. Lupi, S., "Planar circular coils for induction heating," *Electrowarm International*, Vol. 37, No. 9, 319–326, 1979.
19. Carretero, C., et al., "Modeling mutual impedances of non-coaxial inductors for induction heating applications," *IEEE Trans. Magn.*, Vol. 44, No. 11, 4115–4118, 2008.
20. Burke, S. K. and M. E. Ibrahim, "Mutual impedance of air-cored coils above a conducting plate," *J. Phys. D: Appl. Phys.*, Vol. 37, No. 13, 1857–1868, 2004.
21. Michalski, K. A. and R. D. Nevels, "On the use of the coulomb gauge in solving source-excited boundary value problems of electromagnetics," *IEEE Trans. Microwave Theory Tech.*, Vol. 36, No. 9, 1328–1333, 1988.
22. Tsang, L., et al., "Evaluation of the Green's function for the mixed potential integral equation (MPIE) method in the time domain for layered media," *IEEE Trans. Antennas Propag.*, Vol. 51, No. 7, 1559–1571, 2003.
23. Dreher, A., "A new approach to dyadic Green's function in

- spectral domain,” *IEEE Trans. Antennas Propag.*, Vol. 43, No. 11, 1297–1302, 1995.
24. Weiss, S. J. and O. Kilic, “A vector transform solution procedure for solving electromagnetic problems in cartesian coordinates,” *IEEE Antennas Wireless Propag. Lett.*, Vol. 9, 291–294, 2010.
 25. Chew, W. C., *Waves and Fields in Inhomogeneous Media*, IEEE Press, New York, 1995 (reprint from the original from 1990).
 26. Dural, G. and M. I. Aksun, “Closed-form Green’s functions for general sources and stratified media,” *IEEE Trans. Microwave Theory. Tech.*, Vol. 43, No. 7, 1545–1552, 1995.
 27. Michalski, K. A. and J. R. Mosig, “Multilayered media Green’s functions in integral equation formulations,” *IEEE Trans. Antennas Propag.*, Vol. 45, No. 3, 508–519, 1997.
 28. Sadiku, M. N. O., *Numerical Techniques in Electromagnetics*, CRC Press, Boca Raton, 2000.
 29. Chew, W. C. and T. M. Habashy, “The use of vector transforms in solving some electromagnetic scattering problems,” *IEEE Trans. Antennas Propag.*, Vol. 34, No. 7, 871–879, 1986.
 30. Edminister, J. E., *Theory and Problems of Electric Circuits*, Schaum, New York, 1965.